OPEN

NPG Asia Materials (2017) 9, e411; doi:10.1038/am.2017.108
www.nature.com/am

ORIGINAL ARTICLE

Universal high work function flexible anode for simplified ITO-free organic and perovskite light-emitting diodes with ultra-high efficiency

Su-Hun Jeong[1,4], Seong-Hoon Woo[1,4], Tae-Hee Han[2], Min-Ho Park[1], Himchan Cho[2], Young-Hoon Kim[2], Hyunsu Cho[3], Hobeom Kim[1], Seunghyup Yoo[3] and Tae-Woo Lee[2]

Flexible transparent electrode materials such as conducting polymers, silver nanowires, carbon nanotubes and graphenes are being investigated as possible replacements for conventional brittle inorganic electrodes. However, they have critical drawbacks of low work function (WF), resulting in a high hole injection barrier to an overlying semiconducting layer in simplified organic or organic–inorganic hybrid perovskite light-emitting diodes (OLEDs or PeLEDs). Here, we report a new anode material (AnoHIL) that has multifunction of both an anode and a hole injection layer (HIL) as a single layer. The AnoHIL has easy WF tunability up to 5.8 eV and thus makes ohmic contact without any HIL. We applied our anodes to simplified OLEDs, resulting in very high efficiency (62% ph el^{-1} for single and 88% ph el^{-1} for tandem). The AnoHIL showed a similar tendency in simplified PeLEDs, implying universal applicability to various optoelectronics. We also demonstrated large-area flexible lightings using our anodes. Our results provide a significant step toward the next generation of high-performance simplified indium tin oxide (ITO)-free light-emitting diodes.

NPG Asia Materials (2017) **9,** e411; doi:10.1038/am.2017.108; published online 28 July 2017

INTRODUCTION

Optoelectronic devices require a transparent conductive electrode through which visible light emits in light-emitting diodes (LEDs) or through which light can strike a photoactive layer to create electricity in solar cells.[1,2] Inorganic metal oxides such as indium tin oxide (ITO) have been the most common transparent electrode material for conventional commercialized optoelectronic electronics.[3] However, the main disadvantages of conventional ITO electrodes, such as brittleness, increasing cost because of gradual depletion of raw materials, release of metallic indium and tin species into overlying layers[4] and low transparency in the blue, impose a serious limitation on their use in flexible optoelectronic device applications. Therefore, a mechanically stable and flexible electrode capability should be realized to enable fabrication of flexible optoelectronic devices. As ITO is typically used for anodes, it is critical to develop flexible transparent anodes with good hole injection capabilities. At the same time, minimizing the manufacturing cost by simplifying the device structure is also a very critical issue for commercialization. In these respects, universally applicable and versatile flexible electrodes with multifunction will be very useful in various simplified optoelectronics.

Some types of flexible anodes have already been developed, including conducting polymers, silver nanowires, carbon nanotubes and graphenes.[4–31] However, research on flexible anodes to date has been focused mainly on their electrical properties (that is, reduction of sheet resistance), and little care has been taken for their electronic properties: one of the most serious concerns is that these flexible electrodes often suffer from low work function (WF) (highly conductive polymers: 4.5–5.0 eV,[10–16] silver nanowires: 4.2–4.3 eV,[19] carbon nanotubes[21–23]/graphenes:[4,25–27] 4.4–4.6 eV) that give rise to hole injection problem in optoelectronic devices. For example, solution-processed conducting polymers represented by poly (3,4-ethylenedioxythiophene):polystyrene sulfonate (PEDOT:PSS) are being spotlighted as next-generation flexible and stretchable transparent electrodes.[30] In the PEDOT:PSS, PEDOT is a conducting polymer with π–π conjugation in its main backbone. PSS is a primary dopant to increase the hole carrier density of PEDOT by removing electrons from PEDOT. However, for PEDOT:PSS to be used as electrodes, its electrical conductivity should be improved by an additional dopant or chemical post treatments. The post treatments remove the excess insulating PSS chains in PEDOT:PSS films by immersing them into polar solvents[11] or acid,[31] improving the π–π stacking of PEDOT

[1]Department of Materials Science and Engineering, Pohang University of Science and Technology (POSTECH), Gyungbuk, Republic of Korea; [2]Department of Materials Science and Engineering, Seoul National University, Seoul, Republic of Korea and [3]Department of Electrical Engineering, Korea Advanced Institute of Science and Technology (KAIST), Daejeon, Republic of Korea
[4]These two authors contributed equally to this work.
Correspondence: Professor T-W Lee, Department of Materials Science and Engineering, Seoul National University, Engineering Building 33, Room 316, 1 Gwanak-ro, Gwanak-gu, Seoul 08826, Republic of Korea.
E-mail: twlees@snu.ac.kr
Received 2 March 2017; revised 4 April 2017; accepted 5 April 2017

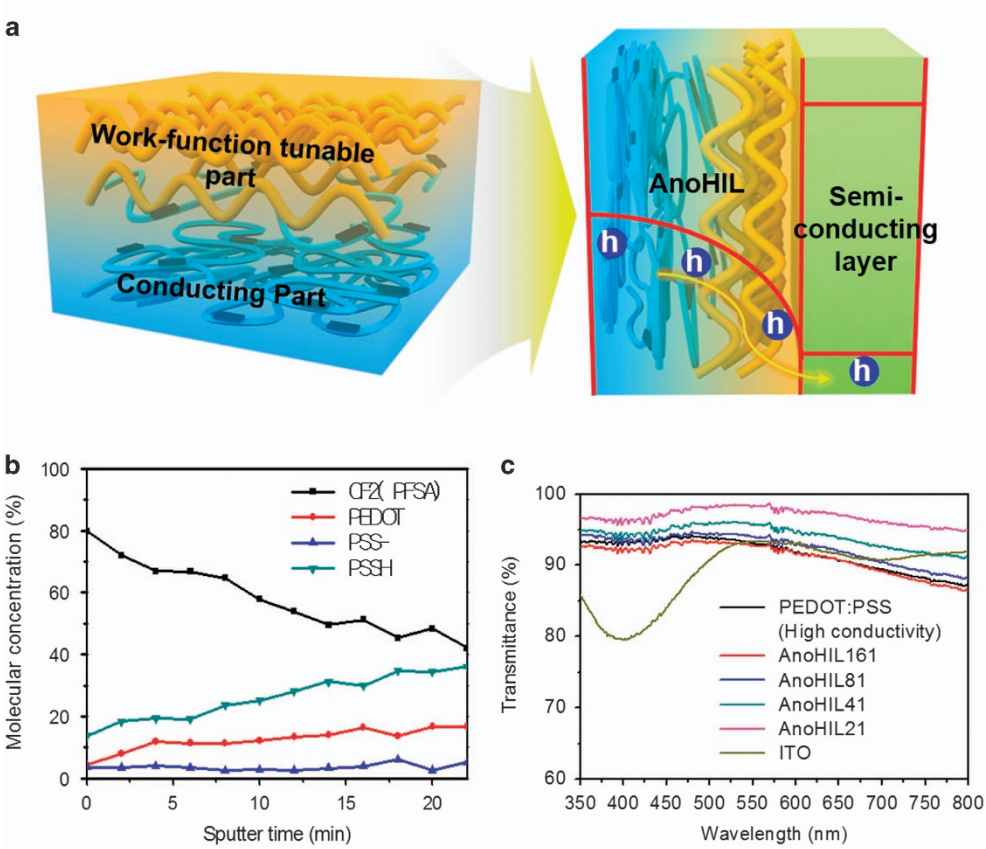

Figure 1 (**a**) The schematics of spin-coated implying combination of anode and HIL (AnoHIL) film that shows self-organization and hole injection from the AnoHIL film to an overlying organic layer. (**b**) Molecular depth profile of AnoHIL21. Three deconvoluted S 2*p* peaks and C 1*s* peak were used for assigning PEDOT, PSS-, PSSH and PFSA, respectively. (**c**) The transmittance of AnoHIL films, conventional indium tin oxide (ITO) and polymeric anode material according to visible regime wavelength. PEDOT, poly(3,4-ethylenedioxythiophene; PFSA, tetrafluoroethylene-perfluoro-3,6-dioxa-4-methyl-7-octenesulphonic acid copolymer; PSS, polystyrene sulfonate.

chains. As a result, the electrical conductivity of PEDOT:PSS films dramatically increased. However, after treatment, the WF of PEDOT:PSS films decreased because of the removal of PSS.[11] The WF of conductivity-increased PEDOT:PSS is 4.8–5.0 eV that is even lower than that of ITO (4.7–5.1 eV), and thus require an additional hole injection layer (HIL) to guarantee device performance comparable to that of devices that use ITO. On the other hand, silver nanowire networks can be used as transparent electrodes because of low sheet resistance (10–50 ohm sq^{-1}). However, the low WF (4.2–4.3 eV), very rough surface and very low surface coverage of silver nanowire networks essentially require additional thick buffer HIL to be used as transparent electrodes in organic light-emitting diodes (OLEDs)[17–19] and organic–inorganic hybrid perovskite light-emitting diodes (PeLEDs).[20] Similarly, carbon-based materials such as carbon nanotubes[21,22] and graphene[4,25–27] are also regarded as candidates for transparent electrodes because of their mechanical strength and flexibility, but they also have low WF (4.4–4.6 eV) and require an additional HIL. Therefore, a highly efficient flexible anode that has high WF should be developed to achieve high-performance simplified flexible optoelectronics at a low cost.

Here, we report on a new concept of flexible universal anode with tunable WF up to 5.8 eV that acts as both anode and HIL with good hole injection capability. Therefore, we name our flexible anode as AnoHIL, implying combination of anode and HIL. This AnoHIL layer is formed by a simple solution process such as spin coating, and shows excellent WF tunability because of self-organization that results in overwhelmingly better device performance than that of OLEDs and PeLEDs on top of ITO. Previously, we have reported a high WF polymeric HIL called as GraHIL.[26] However, the GraHIL has very low conductivity ($<10^{-3}$ S cm^{-1}), and requires essentially an additional conducting anode layer with high conductivity such as ITO and graphene. However, the AnoHIL acts as both anode and HIL and thus does not require an additional conductor, and can simplify the organic or organic–inorganic hybrid device structures including OLEDs and PeLEDs even with highly enhanced device performance. The difference between our AnoHIL and the reported GraHIL is summarized in Supplementary Table S1. To realize our concept, we prepare WF-tunable polymeric compositions composed of a highly conductive polymer, PEDOT:PSS (1 w:2.5 w, CLEVIOS (Hanau, Germany) PH 500) for conduction, and using tetrafluoroethylene-perfluoro-3,6-dioxa-4-methyl-7-octenesulphonic acid copolymer (PFSA) for WF tuning, and a polar organic additive (dimethyl sulfoxide) to increase conductivity that are capable of self-organization to control WF without significant loss of conductivity. Dark injection space charge-limited current (DI-SCLC) measurement clearly demonstrated that the surface-enriched fluorinated ionic polymer can improve the hole injection capability and eventually form ohmic contact to an overlying semiconducting layer. We demonstrated the wide applicability of AnoHILs to various LEDs, including vacuum-deposited green OLEDs, green PeLEDs and large-size white OLEDs for solid-state lighting. The

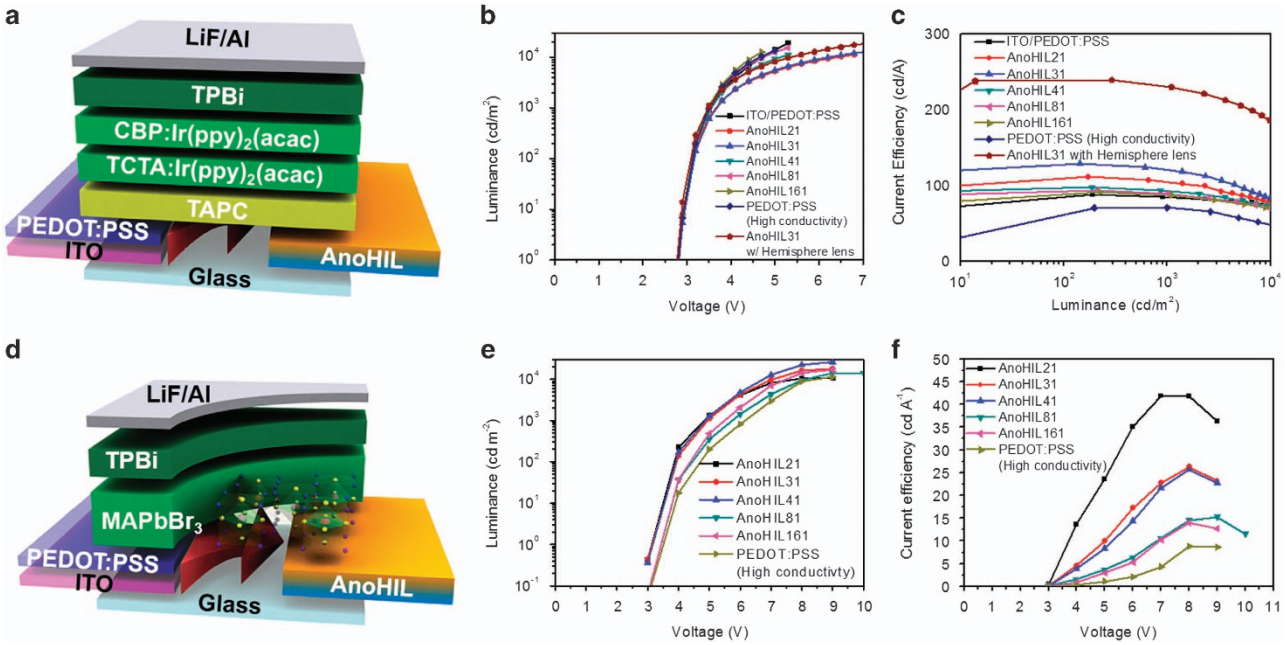

Figure 2 (**a**) The schematic device structure of simplified green phosphorescent organic light-emitting diodes (OLEDs). (**b**) Luminance and (**c**) current efficiency of green phosphorescent OLEDs on top of conventional indium tin oxide (ITO) and AnoHILs. (**d**) The schematic device structure of simplified green perovskite light-emitting diodes (PeLEDs). (**e**) Luminance and (**f**) current efficiency of green PeLEDs on top of different polymeric anodes.

Table 1 Summarization of the simulated spectral power density ratio depending on the position in OLEDs

	Outcoupled	*Substrate*	*Waveguide*	*Surface plasmon*	*Absorption*
ITO/PEDOT:PSS	23.73%	22.57%	30.43%	6.95%	16.32%
AnoHIL31	30.29%	31.08%	27.79%	5.17%	5.67%
PEDOT:PSS	26.17%	30.01%	26.26%	8.40%	9.14%

Abbreviations: ITO, indium tin oxide; OLED, organic light-emitting diode; PEDOT:PSS, poly(3,4-ethylenedioxythiophene):polystyrene sulfonate.

AnoHILs with high WFs in OLEDs and PeLEDs resulted in extremely high device efficiencies (for single unit simplified OLED, 239 cd A^{-1} and 62% ph el^{-1} with a hemisphere lens; for tandem OLEDs, 415 cd A^{-1}, 88% ph el^{-1} with a hemisphere lens; for PeLEDs, 42 cd A^{-1}, 8.66% ph el^{-1} without a hemisphere lens).

MATERIALS AND METHODS

Green phosphorescent OLED fabrication

Before deposition of polymeric and organic materials, glass substrates were cleaned in acetone for 15 min and in isopropyl alcohol for 15 min by sonication. On top of the glass substrate, our polymeric anode materials, AnoHILs composed of highly conductive PEDOT:PSS (CLEVIOS PH 500), PFSA (527084, Sigma-Aldrich Co., St Louis, MO, USA) as a fluorinated ionic polymer and 5 wt% of dimethyl sulfoxide (Junsei Chemical Co., Tokyo, Japan) additive, were spin-coated to have 100 nm thickness, and were then baked on a hot plate at 200 °C for 10 min in air. After transferring the specimen to vacuum thermal evaporators, Di-[4-(*N*,*N*-ditolyl-amino)-phenyl] cyclohexane (TAPC) (15 nm) was deposited as a hole transporting layer (HTL). The green-emitting dopant material bis(2-phenylpyridine)(acetylacetonato)iridium(III) ($Ir(ppy)_2$(acac)) was doped into two different layers (5 nm for each) with 1,1-bis [4-[*N*,*N*-di (p-tolyl) amino]phenyl]cyclohexane (TCTA) and 4,4′-*N*,*N*′-dicarbazolylbiphenyl (CBP) as the host materials, respectively. The host/dopant ratios of TCTA/$Ir(ppy)_2$(acac) and CBP/$Ir(ppy)_2$(acac) were 97:3 (v/v) and 97:4 (v/v), respectively. 1,3,5-tri (phenyl-2-benzimidazolyl)-benzene (TPBi) (65 nm) was used as an ETL. A cathode layer of lithium fluoride (LiF) (1 nm)/Al (110 nm) was deposited under high vacuum ($<5\times10^{-7}$ Torr).

For the comparative study, OLED devices were fabricated with a conventional polymeric HIL, PEDOT:PSS (CLEVIOS P VP AI4083). Except for polymeric anode materials and PEDOT:PSS, all other materials were thermally deposited under high vacuum condition.

Green PeLED fabrication

The methylammonium lead bromide ($MAPbBr_3$) solution (40 wt%) was prepared by dissolving MABr and $PbBr_2$ with a molar ratio of MABr/$PbBr_2$ =1.06:1 in dimethyl sulfoxide while stirring. The AnoHILs on the glass substrate were prepared using the same method used in the OLED fabrication. The AnoHIL samples were transferred into a N_2-filled glove box and the $MAPbBr_3$ solutions were spin-coated in the glove box. During the spin-coating, TPBi in chloroform was dripped. After transferring the AnoHIL/$MAPbBr_3$ samples to a vacuum thermal evaporator, TPBi (50 nm), LiF (1 nm) and Al (100 nm) were deposited in sequence. The devices were encapsulated with a photocurable epoxy resin and a glass lid before exposing them to air.

Green phosphorescent tandem OLED fabrication

The AnoHILs on the glass substrate were prepared using same method used in green fluorescent OLED fabrication. After transferring the specimen to vacuum thermal evaporators, a 15 nm-thick TAPC was deposited as a HTL. The green-emitting dopant material $Ir(ppy)_2$(acac) was doped into two different layers (5 nm for each) with TCTA and CBP as the host materials, respectively. The host/dopant ratios of TCTA/$Ir(ppy)_2$(acac) and CBP/$Ir(ppy)_2$(acac) were 97:3(v/v) and 97:4(v/v), respectively. TPBi (65 nm) was used as an ETL. As a charge generation layer, bathocuproine doped with Ca (20 nm,

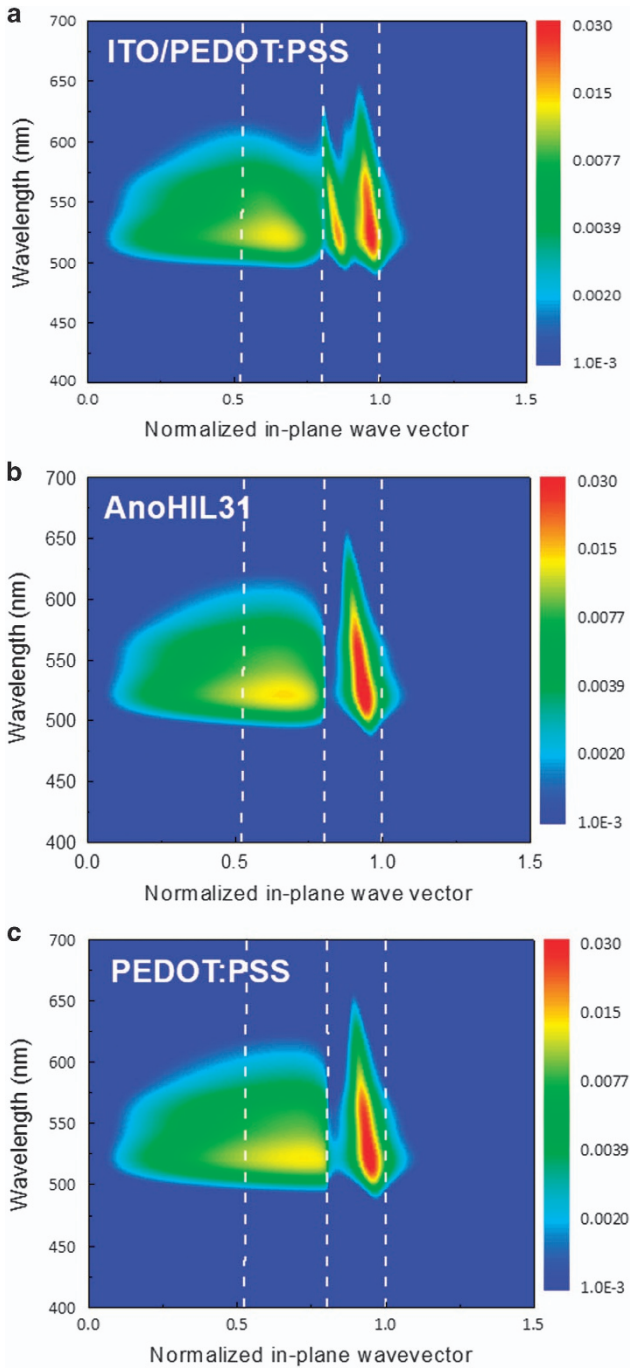

Figure 3 Simulated spectral power density of (**a**) ITO/PEDOT:PSS, (**b**) AnoHIL and (**c**) PEDOT:PSS anode-based green phosphorescent OLEDs. ITO, indium tin oxide; OLED, organic light-emitting diode; PEDOT:PSS, poly(3,4-ethylenedioxythiophene):polystyrene sulfonate

90:10 (v/v)), MoO_3 (5 nm) and TAPC (55 nm) was subsequently deposited. For a second emitting layer, TCTA/$Ir(ppy)_2(acac)$ (5 nm, 97:3 (v/v)) and CBP/$Ir(ppy)_2(acac)$ (5 nm, 97:4 (v/v)) were also deposited. TPBi (65 nm) was used as an ETL, and cathode layers of LiF (1 nm)/Al (110 nm) were deposited under high vacuum ($<5\times10^{-7}$ Torr).

For the comparative study, OLED devices were fabricated with a conventional polymeric HIL, PEDOT:PSS (CLEVIOS P VP AI4083). Except for polymeric anode materials and PEDOT:PSS, all other materials were thermally deposited under high vacuum condition.

Light-emitting diode performance measurement

For performance analysis, the current–voltage–luminescence characteristics have been measured using the Keithley (Cleveland, OH, USA) 236 source measurement unit and a Minolta (Tokyo, Japan) CS2000 spectroradiometer. Device lifetime was measured using a McScience (Suwon, South Korea) Polaronix OLED Lifetime Test System.

RESULTS AND DISCUSSION

Figure 1a shows the schematic image of our polymeric anode material, AnoHIL, and hole injection from the anodes to an overlying semiconducting layer. Because PFSA tends to be enriched on the surface of the polymeric film because of its low surface energy, the AnoHIL layer self-organizes to form two different functional parts (Figure 1a).[32,33] The lower part of the film consists mostly of PEDOT:PSS (1 w:2.5 w, CLEVIOS PH 500) that has higher conductivity and lower WF than the upper part, and it performs sufficiently as an anode of OLEDs and PeLEDs. The upper part near the surface has lower conductivity and much higher WF than the lower part, and hence acts as a HIL in OLEDs and PeLEDs. Thus, this new, single-layer polymeric anode system serves as both anode and HIL in OLED and PeLED devices. To control the surface WF, six kinds of polymeric compositions were prepared with different proportions of each component PFSA (Supplementary Table S2). As the PFSA portion increased, the surface WF tended to increase (Supplementary Table S2). The AnoHIL21 achieved a very high WF of 5.8 eV, and this is to our knowledge the highest WF value among flexible anodes reported to date. To analyze the molecular depth profile of the AnoHIL film to prove the self-organization of PFSA toward the film surface, we used X-ray photoelectron spectroscopy (Supplementary Table S3). The S 2*p* spectrum of PEDOT:PSS was deconvoluted into three peaks (164.5, 168.4 and 168.9 eV) that correspond to PEDOT, PSS-salt and polystyrene sulfonic acid (PSSH), respectively. We also identified the 292 eV peak of the C 1*s* spectrum as the CF_2 bond in PFSA.[34,35] PFSA is clearly highest on the surface of the anode layer and decreases with depth; this is evidence that the PFSA self-organizes to form the gradient AnoHIL film (Figure 1b). We also used the results of X-ray photoelectron spectroscopy analysis to calculate the surface molecular distribution of AnoHILs (Supplementary Table S3). The driving force for the self-organization is the surface energy difference between PFSA and PEDOT:PSS. The PFSA with fluorocarbon chains has lower surface energy (~20 mN m^{-1}) compared with that of PEDOT:PSS (ca., 71–73 mN m^{-1}). The incompatibility of fluorocarbon chains in the PFSA with the hydrocarbon chains in PEDOT:PSS induced phase separation between PFSA and PEDOT:PSS.[36] As a result, the PFSA is preferentially positioned at the surface of AnoHIL film. In the atomic force microscope images, the root mean square roughness of AnoHIL films was lower than PEDOT:PSS (High conductivity) film without PFSA (Supplementary Figure S1). It is attributed to the surface-enriched PFSA molecules. This self-organization of the polymeric blend increases WF and thus facilitates hole injection in OLEDs and PeLEDs. To achieve a successful transparent anode replacement in industry, this layer should also provide high transparency throughout visible range. In the past few decades, OLED devices have been highlighted for general solid-state lighting based on white OLEDs (WOLEDs), and hence the limited blue-region transparency of ITO electrodes is a critical drawback for practical use, and thus increasing the transparency of anode has become an increasingly significant objective. As the AnoHILs had >90% transparency in the entire visible region (Figure 1c), AnoHILs can minimize optical loss and thus increase current efficiency (CE).

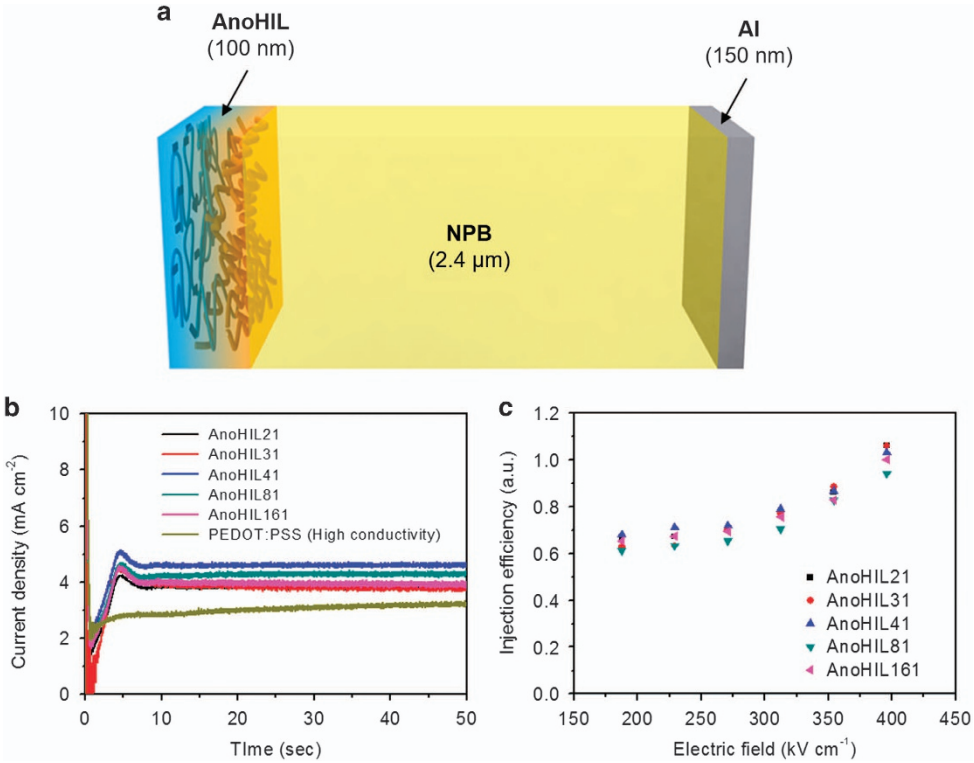

Figure 4 Dark injection space-charge limited current analysis for determining hole mobility and contact property at interfaces. (**a**) Structure of hole-only devices. (**b**) Current density signal that shows contact property between AnoHIL and *N*′-diphenyl-*N*,*N*′-bis(1-napthly)-1,1′-biphenyl-4,4′-diamine (NPB) layer. (**c**) The calculated injection efficiency from AnoHIL anodes.

ITO-based conventional OLED structure can be simplified by employing the AnoHIL anode and removing the overlying HIL (Figure 2a). We also fabricated extremely efficient phosphorescent green OLEDs using the AnoHIL anode, in which the emitting dopant was $Ir(ppy)_2(acac)$, and compared them with ITO devices that used a conventional polymeric HIL, PEDOT:PSS (1 w:6 w, CLEVIOS PV P AI4083) (Figure 2a and Supplementary Figure S2a). The luminance of all devices exceeded 10 000 cd m^{-2} (Figure 2b). The conventional ITO/PEDOT:PSS anode-based OLED had the highest CE = 88 cd A^{-1}. When the AnoHILs were employed, the AnoHIL31 anode-based one had the highest CE = 128 cd A^{-1} (Figure 2c). This device showed high CE of 98 cd A^{-1} at 1000 cd m^{-2} and 83 cd A^{-1} at 10 000 cd m^{-2} (Supplementary Table S4). All the AnoHIL-based OLEDs showed higher maximum CE (91, 93, 98 and 111 cd A^{-1} for AnoHIL 161, 81, 41 and 21, respectively) than the conventional ITO/PEDOT:PSS (anode/HIL bilayer)-based OLED (the highest CE = 88 cd A^{-1}) and PEDOT:PSS (high conductivity) anode-based OLED (the highest CE = 71 cd A^{-1}) (Figure 2c). The highest external quantum efficiency (EQE) of phosphorescent green OLED fabricated with AnoHIL anodes was 33% (for AnoHIL31) (Supplementary Figure S2b) that is much higher than that of the ITO/PEDOT:PSS device (the highest EQE = 20% ph el^{-1}). Supplementary Figure S2c shows the angular emission profiles of the extracted light from the green phosphorescent OLEDs based on ITO/PEDOT:PSS and AnoHIL. The angular emission profile of the AnoHIL device closely resembles the Lambertian emission profile compared with that of the ITO device.

The optical enhancement obtained with the AnoHIL anode was simulated by means of an advanced classical electromagnetic theory following a formalism summarized by Furno *et al.*[37] The distribution of simulated spectral power density clearly shows the optical advantage of OLEDs with the proposed electrodes (Table 1 and Figure 3); the refractive indices of AnoHIL and PEDOT:PSS anode are far smaller than those of ITO electrodes and organic layers and are closer to that of glass substrates (Supplementary Figure S3). This results in a thinner 'core' of waveguides for AnoHIL (Figure 3b) or PEDOT:PSS anode-based OLEDs (Figure 3c) than for ITO/PEDOT:PSS-based OLEDs (Figure 3a), decreasing the overall power coupled to wave-guided modes in OLEDs with the proposed electrodes. Lower absorption of AnoHILs than ITO and PEDOT:PSS electrodes is also noted. Both of these features tend to enhance the sum of outcoupled and substrate-confined modes in the proposed devices. Measurement using a hemi-spherical lens, whose refractive index is matched to that of a glass substrate and thus can extract most of the substrate confined modes, indicates that OLEDs with AnoHIL31 anodes exhibit the maximum CE as high as 239 cd A^{-1} (Figure 2c) and the maximum EQE as high as 62% ph el^{-1} (Supplementary Figure S2b), supporting the notion mentioned above and illustrating that OLEDs with the proposed electrodes can further be advantageous when used with an external structure like a micro-lens array that can extract substrate-confined modes.

PeLEDs have been spotlighted as next-generation light-emitting diodes because of their high color purity and low production cost.[38–40] Green organic–inorganic hybrid perovskite emitters, $MAPbBr_3$, were used as a light-emission layer, and polymeric anodes, including AnoHIL and PEDOT:PSS (high conductivity), were used as anodes (Figure 2d and Supplementary Figure S4a). The AnoHILs showed a similar effect on the CE of PeLEDs. The resultant maximum CEs and EQEs of PeLEDs on top of various polymeric anodes increased up to 42 cd A^{-1} and 8.66% ph el^{-1} for the AnoHIL21-based PeLED as the ratio of PFSA in polymeric anodes increased (26 cd A^{-1},

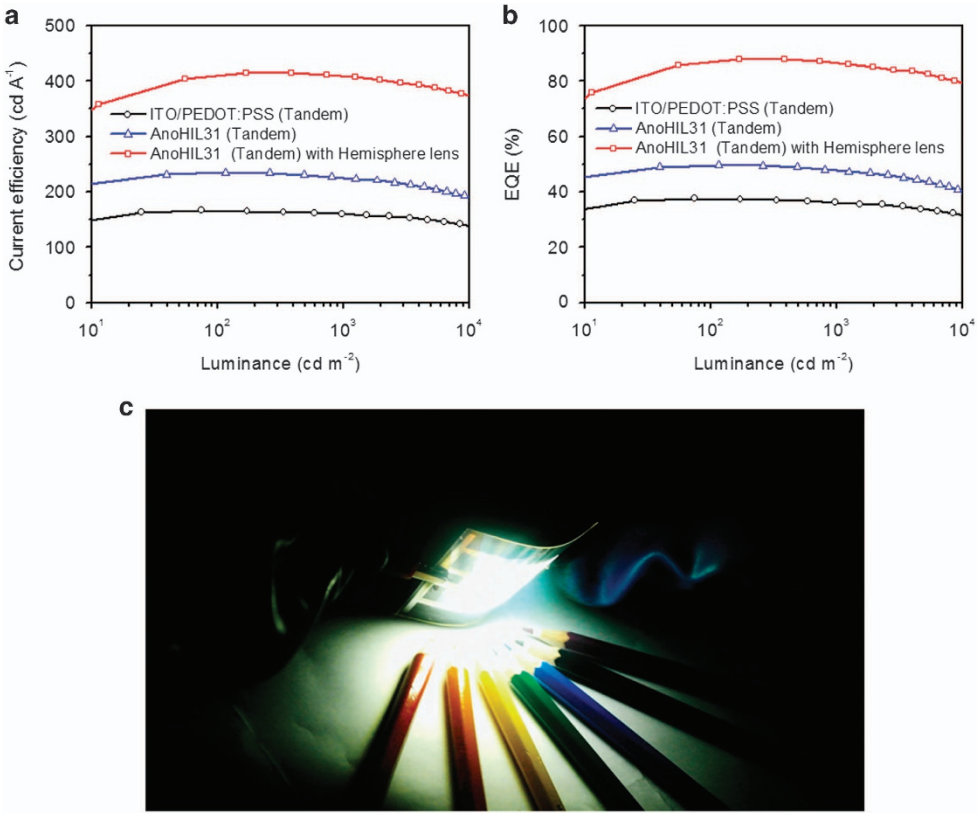

Figure 5 Green phosphorescent tandem organic light-emitting diode (OLED) device characteristics using AnoHIL anodes, and demonstration of large-area general lighting. (**a**) Current efficiency and (**b**) external quantum efficiency (EQE) of green phosphorescent tandem OLEDs fabricated on indium tin oxide (ITO) and AnoHIL anodes. (**c**) The demonstration of large-area white OLED (WOLED) and its operation at 10 V.

5.40% ph el^{-1} for AnoHIL31; 26 cd A^{-1}, 5.30% ph el^{-1} for AnoHIL41; 15 cd A^{-1}, 3.14% ph el^{-1} for AnoHIL81; 14 cd A^{-1}, 2.94% ph el^{-1} for AnoHIL161; and 9 cd A^{-1}, 1.95% ph el^{-1} for PEDOT:PSS (high conductivity) (Figure 2f, Supplementary Table S5 and Supplementary Figure S4c). The angle-dependent emission profile of our PeLEDs was very similar to Lambertian,[39] and the accurate EQEs were calculated from the emission profile. All the PeLEDs produced the very narrow electroluminescence spectra at ~540 nm; full width at half maximum was ~20 nm for all samples (Supplementary Figure S4b). As the surface WF of polymeric anodes decreased, the turn-on voltages at 1 cd m^{-2} increased from 3.19 to 3.51 V (3.19 V for AnoHIl21, 3.20 V for AnoHIl31, 3.23 V for AnoHIl41, 3.44 V for AnoHIL81, 3.45 V for AnoHIL161 and 3.51 V for PEDOT:PSS (high conductivity)) (Figure 2e). It supports that our new polymeric anodes reduce the hole injection barrier from anodes and to $MAPbBr_3$ layers with a very high ionization energy (IE ~ 5.89 eV) (Supplementary Figure S4a).[39]

In addition, the surface-enriched insulating PFSA blocks electrons from cathodes and suppresses exciton quenching at the anode and $MAPbBr_3$ interface.[40,41] The $MAPbBr_3$ film on top of PEDOT:PSS (high conductivity), which directly contacted with the overlying $MAPbBr_3$ layer without the insulating PFSA, showed very short photoluminescence lifetime, and the photoluminescence lifetime was dramatically increased as the PFSA in AnoHIL increased (Supplementary Table S6 and Supplementary Figure S5). The variation of polymeric anodes did not influence the crystal structures of the overlying MAPbBr layer (Supplementary Figure S6). Therefore, we conclude that the enhanced PL lifetime was attributed to prevention of the exciton quenching at the anode/$MAPbBr_3$ interface by surface-enriched PFSA.

The optical simulation does support the efficiency enhancement in OLED with the proposed electrodes to some degree, but the difference expected by pure optical origins is not large enough to provide a full picture. In particular, the measured EQEs of ITO/PEDOT:PSS or PEDOT:PSS (high conductivity) anode-based device are smaller than those predicted by optical simulation, indicating that PEDOT:PSS (high conductivity) anode on its own has a limited injection. To check this in more detail, we used the DI-SCLC measurement to evaluate the contact property between AnoHILs and the overlying hole transport layer, *N*′-diphenyl-*N*,*N*′-bis(1-napthly)-1,1′-biphenyl-4,4′-diamine (NPB) with the structure of AnoHILs (100 nm)/NPB (2400 nm)/Al (100 nm) (Figure 4a). DI-SCLC transient signals were obtained from devices at a constant bias of 8 V; all AnoHIL-based devices exhibited the DI-SCLC transient signal peak, whereas the device using the PEDOT:PSS (High conductivity) anode did not (Figure 4b). The peak appears in the DI-SCLC transient signal only when ohmic contact is fully established,[42–44] and hence each AnoHIL layer clearly formed ohmic contact with the overlying organic layer. We calculated the hole injection efficiency η of each device by the following equation:

$$\eta = \frac{J_{\text{transit}}}{1.2 \times J_{\text{SCL}}} \quad (1)$$

where J_{transit} is the current density measured at the peak of the DI-SCLC transient formed by ohmic contact and J_{SCL} is theoretical

space charge limited current.[44]

$$J_{SCL} = \frac{9}{8}\varepsilon\varepsilon_0\mu_0 \exp(0.8918\beta\sqrt{V/d})\frac{V^2}{d^3} \quad (2)$$

where ε is the dielectric constant, ε_0 is the vacuum permittivity, V is the voltage applied, d is the film thickness, μ_0 is the mobility when electric field is zero and β is the Poole–Frenkel constant that is responsible for electric field-dependent carrier mobility in disordered or amorphous materials. The calculated hole injection efficiency of AnoHIL21-AnoHIL41 as a function of electric field showed nearly ohmic contact ($\eta \sim 1$) (Figure 4c) because the AnoHIL WF levels are deeper than highest occupied molecular orbital of the overlying semiconducting layer (NPB) (~5.4 eV). These results are consistent with our experimental results and re-confirm the notion of hole-injection improvement obtained with AnoHIL.

We also fabricated a green phosphorescent tandem OLED with a simplified structure using the AnoHIL anode (AnoHIL31), in which the charge generation layer was bathocuproine doped with Ca (20 nm, 90:10 (v/v))/MoO_3 (5 nm)/TAPC (55 nm) and compared with the ITO devices that used a conventional polymeric HIL, PEDOT:PSS (CLEVIOS PV P AI4083) (Supplementary Figure S7). The conventional ITO/PEDOT:PSS-based tandem OLED had the highest CE = 167 cd A^{-1}. When the AnoHIL31 was employed, the simplified tandem OLED had the highest CE = 235 cd A^{-1} (Figure 5a), the highest current efficiency ever reported up to date in tandem OLEDs without an outcoupling structure. The EQE of the green phosphorescent tandem OLED fabricated on the AnoHIL31 anode was 50% (Figure 5b), much higher than that of the ITO/PEDOT:PSS anode tandem device (the highest EQE = 38%). The accurate EQEs were calculated from the emission profile (Supplementary Figure S8). Measurement using a hemi-spherical lens indicates that the OLED with the AnoHIL31 anode exhibits the maximum CE as high as 415 cd A^{-1} (Figure 5a) (the highest EQE = 88% ph el^{-1} (Figure 5b) with low efficiency roll-off (by 10% at 10 000 cd m^{-2}) (Supplementary Table S4).

One of eventual goals of OLED production is the commercialization of general solid-state lighting. Here, we fabricated highly efficient simplified phosphorescent WOLEDs by using an AnoHIL anode (Supplementary Figure S9a). To achieve white emission, two complementarily emitting dopants of the sky-blue phosphor, bis(4,6-difluorophenylpyridinato-*N*, $C^{2'}$)(picolinate)iridium(III) (FIrpic) and the orange-red phosphor, bis(2-phenylbenzothiozolato-*N*,$C^{2'}$)iridium(III) (acetylacetonate) (Bt2Ir(acac)) were used. In the electroluminescence spectra of the AnoHIL31 device at 6.3 V, FIrpic produced a peak at 471 nm and Bt2Ir(acac) produced a peak at 557 nm (Supplementary Figure S9c). The WOLED device fabricated on AnoHIL31 had a high maximum CE = 56.39 cd A^{-1} (Supplementary Figure S9b). In comparison, the device using an ITO electrode and a PEDOT:PSS HIL had a maximum CE = 32.43 cd A^{-1}. This high improvement in CE using the AnoHIL anode can be attributed to the high transmittance throughout visible range and the lowered hole injection barrier between the anode and the overlying organic layer. In addition, to demonstrate the feasibility of using AnoHILs in large-area flexible general lighting, we fabricated large-area (3×3.5 cm^2) flexible WOLEDs on a flexible polyethylene teraphthalate substrate (5×5 cm^2). The device structure is indicated in Supplementary Figure S10. We achieved bright uniform lighting from large-area flexible WOLED at 10 V (Figure 5c); this result is an evidence of the feasibility of using AnoHILs in flexible solid-state general lighting. We are confident that our results provide a significant step for realization of flexible WOLED.

CONCLUSION

In conclusion, we developed a versatile and universal flexible conducting polymer anode, AnoHIL, that can tune WF up to 5.8 eV and prevent exciton quenching and significantly increase CE of simplified OLEDs and PeLEDs in a single junction even without an additional HIL. Furthermore, the phosphorescent green tandem OLED fabricated on the AnoHIL anode had an extremely high record efficiency of 415 cd A^{-1} and 88% ph el^{-1}. The AnoHIL anode also showed the similar effect on simplified PeLEDs: significant increase of electroluminescence efficiency with a function of PFSA. In addition, we also successfully demonstrated a large (3×3.5 cm^2) flexible AnoHIL-based WOLED on a (5×5 cm^2) polyethylene teraphthalate substrate. DI-SCLC measurement clearly exhibited that ohmic contact was well established between the anode and the overlying semiconducting layer. WF-tunable flexible anodes such as those presented here have a great potential for realization of high-performance flexible organic or organic–inorganic hybrid perovskite electronic and optoelectronic devices with a simplified structure.

CONFLICT OF INTEREST

The authors declare no conflict of interest.

ACKNOWLEDGEMENTS

This research was supported by the Nano Material Technology Development Program through the National Research Foundation of Korea (NRF) funded by the Ministry of Science, ICT & Future Planning (MSIP, Korea) (NRF-2014M3A7B4051747). This work was also supported by the National Research Foundation of Korea (NRF) grant funded by the Korea government (Ministry of Science, ICT & Future Planning) (NRF-2016R1A3B1908431). S-HJ gratefully acknowledges financial support by Global PhD Fellowship Program through the National Research Foundation of Korea (NRF) funded by the Ministry of Education (NRF-2012H1A2A1002581).

PUBLISHER'S NOTE

1 Tang, C. W. & VanSlyke, S. A. Organic electroluminescent diodes. *Appl. Phys. Lett.* **51**, 913–915 (1987).
2 Gustafsson, G., Cao, Y., Treacy, G. M., Klavetter, F., Colaneri, N. & Heeger, A. J. Flexible light-emitting diodes made from soluble conducting polymers. *Nature* **357**, 477–479 (1992).
3 Kumar, A. & Zhou, C. The race to replace tin-doped indium oxide: which material will win? *ACS Nano* **4**, 11–14 (2010).
4 Seo, H.-K., Kim, H., Lee, J., Park, M.-H., Jeong, S.-H., Kim, Y.-H., Kwon, S.-J., Han, T.-H., Yoo, S. & Lee, T.-W. Efficient flexible organic/inorganic hybrid perovskite light-emitting diodes based on graphene anode. *Adv. Mater.* **29** (2017).
5 Huang, J., Miller, P. F., Wilson, J. S., de Mello, A. J., de Mello, J. C. & Bradley, D. D. Investigation of the effects of doping and post-deposition treatments on the conductivity, morphology, and work function of poly (3,4-ethylenedioxythiophene)/poly (styrene sulfonate) films. *Adv. Funct. Mater.* **15**, 290–296 (2005).
6 Kim, J. Y., Jung, J. H., Lee, D. E. & Joo, J. Enhancement of electrical conductivity of poly(3,4-ethylenedioxythiophene)/poly(4-styrenesulfonate) by a change of solvents. *Synth. Met.* **126**, 311–316 (2002).
7 Pettersson, L. A., Ghosh, S. & Inganäs, O. Optical anisotropy in thin films of poly(3,4-ethylenedioxythiophene)/poly(styrene sulfonate). *Org. Electron.* **3**, 143–148 (2002).
8 Ouyang, J., Chu, C. W., Chen, F. C., Xu, Q. & Yang, Y. High-conductivity poly (3,4-thylenedioxythiophene):poly (styrene sulfonate) film and its application in polymer optoelectronic devices. *Adv. Funct. Mater.* **15**, 203–208 (2005).
9 Huang, J., Wang, X., Kim, Y. & Bradley, D. D. C. High efficiency flexible ITO-free polymer/fullerene photodiodes. *Phys. Chem. Chem. Phys.* **8**, 3904–3908 (2006).
10 Admassie, S., Zhang, F., Manoj, A. G., Svensson, M., Andersson, M. R. & Inganäs, O. A polymer photodiode using vapour-phase polymerized PEDOT as an anode. *Sol. Energy Mater. Sol. Cells* **90**, 133–141 (2006).
11 Fehse, K., Walzer, K., Leo, K., Lövenich, W. & Elschner, A. Highly conductive polymer anodes as replacements for inorganic materials in high-efficiency organic light-emitting diodes. *Adv. Mater.* **19**, 441–444 (2007).

12 Na, S. I., Kim, S. S., Jo, J. & Kim, D. Y. Efficient and flexible ITO-free organic solar cells using highly conductive polymer anodes. *Adv. Mater.* **20**, 4061–4067 (2008).
13 Worfolk, B. J., Andrews, S. C., Park, S., Reinspach, J., Liu, N., Toney, M. F., Mannsfeld, S. C. B. & Bao, Z. Ultrahigh electrical conductivity in solution-sheared polymeric transparent films. *Proc. Natl. Acad. Sci. USA* **112**, 14138–14143 (2015).
14 Zhou, Y., Fuentes-Hernandez, C., Shim, J., Meyer, J., Giordano, A. J., Li, H., Winget, P., Papadopoulos, T., Cheun, H., Kim, J., Fenoll, M., Dindar, A., Haske, W., Najafabadi, E., Khan, T. M., Sojoudi, H., B. Stephen, B., Graham, S., Brédas, J.-L., Marder, S. R., Kahn, A. & Fenoll, M. A universal method to produce low-work function electrodes for organic electronics. *Science* **336**, 327–332 (2012).
15 Winther-Jensen, B. & Krebs, F. C. High-conductivity large-area semi-transparent electrodes for polymer photovoltaics by silk screen printing and vapour-phase deposition. *Sol. Energy Mater. Sol. Cells* **90**, 123–132 (2006).
16 Levermore, P. A., Chen, L., Wang, X., Das, R. & Bradley, D. D. Fabrication of highly conductive poly(3,4-ethylenedioxythiophene) films by vapor phase polymerization and their application in efficient organic light-emitting diodes. *Adv. Mater.* **19**, 2379–2385 (2007).
17 Yu, Z., Zhang, Q., Li, L., Chen, Q., Niu, X., Liu, X., Liu, J. & Pei, Q. Highly flexible silver nanowire electrodes for shape-memory polymer light-emitting diodes. *Adv. Mater.* **23**, 664 (2011).
18 Yu, Z., Li, L., Zhang, Q., Hu, W. & Pei, Q. Silver nanowire-polymer composite electrodes for efficiency polymer solar cells. *Adv. Mater.* **23**, 4453 (2011).
19 Gaynor, W., Hofmann, S., Christoforo, M. G., Sachse, C., Mehra, S., Salleo, A., McGehee, M. D., Gather, M. C., Lüssem, B., Müller-Meskamp, L., Peumans, P. & Leo, K. Color in the corners: ITO-free white OLEDs with angular color stability. *Adv. Mater.* **25**, 4006–4013 (2013).
20 Bade, S. G. R., Li, J., Shan, X., Ling, Y., Tian, Y., Dilbeck, T., Besara, T., Geske, T., Gao, H., Ma, B., Hanson, K., Siegrist, T., Xu, C. & Yu, Z. Fully printed halide perovskite light-emitting diodes with silver nanowire electrodes. *ACS Nano* **10**, 1795–1801 (2016).
21 Suzuki, S., Bower, C., Watanabe, Y. & Zhou, O. Work functions and valence band states of pristine and Cs-intercalated single-walled carbon nanotube bundles. *Appl. Phys. Lett.* **76**, 4007–4009 (2000).
22 Zhao, J., Han, J. & Lu, J. P. Work functions of pristine and alkali-metal intercalated carbon nanotubes and bundles. *Phys. Rev. B* **65**, 193401 (2002).
23 Ou, E. C., Hu, L., Raymond, G. C. R., Soo, O. K., Pan, J., Zheng, Z., Park, Y., Hecht, D., Irvin, G., Drzaic, P. & Gruner, G. Surface-modified nanotube anodes for high performance light-emitting diodes. *ACS Nano* **3**, 2258–2264 (2009).
24 Wu, J., Agrawal, M., Becerril, H. A., Bao, Z., Liu, Z., Chen, Y. & Peumans, P. Organic light-emitting diodes on solution-processed graphene transparent electrodes. *ACS Nano* **4**, 43–48 (2010).
25 Sun, T., Wang, Z. L., Shi, Z. J., Ran, G. Z., Xu, W. J., Wang, Z. Y., Li, Y. Z., Dai, L. & Qin, G. G. Multilayered graphene used as anode of organic light emitting devices. *Appl. Phys. Lett.* **96**, 133301 (2010).
26 Han, T. H., Lee, Y., Choi, M. R., Woo, S. H., Bae, S. H., Hong, B. H., Ahn, J.-H. & Lee, T. W. Extremely efficient flexible organic light-emitting diodes with modified grapheme anode. *Nat. Photon.* **6**, 105–110 (2012).
27 Li, N., Oida, S., Tulevski, G. S., Han, S. J., Hannon, J. B., Sadana, D. K. & Chen, T. C. Efficient and bright organic light-emitting diodes on single-layer grapheme electrodes. *Nat. Commun.* **4**, 2294 (2013).
28 Kim, H., Bae, S.-H., Han, T.-H., Lim, K.-G., Ahn, J.-H. & Lee, T.-W. Organic solar cells using CVD-grown graphene electrodes. *Nanotechnology* **25**, 014012 (2014).
29 Kim, H., Byun, J., Bae, S.-H., Ahmed, T., Zhu, J.-X., Kwon, S.-J., Lee, Y., Min, S.-Y., Wolf, C., Seo, H.-K., Ahn, J.-H. & Lee, T.-W. On-fabrication solid-state N-doping of graphene by an electron transporting metal oxide layer for efficient inverted organic solar cells. *Adv. Energy Mater.* **6**, 1600172 (2016).
30 Oh, J. Y., Kim, S., Baik, H. K. & Jeong, U. Conducting polymer dough for deformable electronics. *Adv. Mater.* **38**, 4455–4461 (2016).
31 Kim, N., Kee, S., Lee, S. H., Lee, B. H., Kahng, Y. H., Jo, Y. R., Kim, B.-J. & Lee, K. Highly conductive PEDOT:PSS nanofibrils induced by solution-processed crystallization. *Adv. Mater.* **26**, 2268–2272 (2014).
32 Choi, M. R., Han, T. H., Lim, K. G., Woo, S. H., Huh, D. H. & Lee, T. W. Soluble self-doped conducting polymer compositions with tunable work function as hole injection/extraction layers in organic optoelectronics. *Angew. Chem. Int. Ed.* **50**, 6274–6277 (2011).
33 Choudhury, K. R., Lee, J., Chopra, N., Gupta, A., Jiang, X., Amy, F. & So, F. Efficient hole injection in organic light-emitting diodes. *Adv. Funct. Mater.* **19**, 491–496 (2009).
34 Huang, L. M., Tang, W. R. & Wen, T. C. Spatially electrodeposited platinum in polyaniline doped with poly(styrene sulfonic acid) for methanol oxidation. *J. Power Sources* **164**, 519–526 (2007).
35 Susac, D., Kono, M., Wong, K. C. & Mitchell, K. A. R. XPS study of interfaces in a two-layer light-emitting diode made from PPV and Nafion with ionically exchanged Ru $(bpy)_3^{2+}$. *Appl. Surf. Sci.* **174**, 43–50 (2001).
36 Lee, T. W., Chung, Y., Kwon, O. & Park, J. J. Self-organized gradient hole injection to improve the performance of polymer electroluminescent devices. *Adv. Funct. Mater.* **17**, 390–396 (2007).
37 Furno, M., Meerheim, R., Hofmann, S., Lüssem, B. & Leo, K. Efficiency and rate of spontaneous emission in organic electroluminescent devices. *Phys. Rev. B* **85**, 115205 (2012).
38 Tan, Z. K., Moghaddam, R. S., Lai, M. L., Docampo, P., Higler, R., Deschler, F., Price, M., Sadhanala, A., Pazos, L. M., Credgington, D., Hanusch, F., Bein, T., Snaith, H. J. & Friend, R. H. Bright light-emitting diodes based on organometal halide perovskite. *Nat. Nanotechnol.* **9**, 687–692 (2014).
39 Cho, H., Jeong, S. H., Park, M. H., Kim, Y. H., Wolf, C., Lee, C. L., Im, S. H., Friend, R. H. & Lee, T.-W. Overcoming the electroluminescence efficiency limitations of perovskite light-emitting diodes. *Science* **350**, 1222–1225 (2015).
40 Kim, Y. H., Cho, H., Heo, J. H., Kim, T. S., Myoung, N., Lee, C. L., Im, S. H. & Lee, T.-W. Multicolored organic/inorganic hybrid perovskite light-emitting diodes. *Adv. Mater.* **27**, 1248–1254 (2014).
41 Han, T. H., Choi, M. R., Woo, S. H., Min, S. Y., Lee, C. L. & Lee, T.-W. Molecularly controlled interfacial layer strategy toward highly efficient simple-structured organic light-emitting diodes. *Adv. Mater.* **24**, 1487–1493 (2012).
42 Goldie, D. M. Transient space-charge-limited current pulse shapes in molecularly doped polymers. *J. Phys. D Appl. Phys.* **32**, 3058–3067 (1999).
43 Campbell, I. H., Smith, D. L., Neef, C. J. & Ferraris, J. P. Consistent time-of-flight mobility measurements and polymer light-emitting diode current-voltage characteristics. *Appl. Phys. Lett.* **74**, 2809–2811 (1999).
44 Murgatroyd, P. N. Theory of space-charge-limited current enhanced by Frenkel effect. *J. Phys. D Appl. Phys.* **3**, 151 (1970).

Supplementary Information accompanies the paper on the NPG Asia Materials website (http://www.nature.com/am)